Statistical Human Body Shape Model including Elderly People

Yusuke Yoshiyasu[1], Vincent Samy, Yumeko Imamura, Ko Ayusuwa, Ryuusuke Sagawa, Eiichi Yoshida
AIST CNRS-AIST JRL

***Abstract*— In this study, we present a human body shape statistical model including elderly people, which is constructed using principal component analysis (PCA) on 3D body scan data of approximately 130 people. As a pre-process step, a template human body mesh model is fitted to 3D scan data using a coarse-to-fine surface registration technique based on a conformal deformation method, in order to establish correspondences between the scans of different subjects possibly in different poses. To change body style by a small set of parameters, such as "age", "weight" and "height" or the easily measurable anthropometric parameters like "shoulder width", the linear transformations between these attributes and the first 10 principal component scores are obtained. We design a simple user interface to use this deformation model to generate different body styles easily. As a result, we were able to produce and show body styles capturing the characteristics of elderly people whose shoulders fell and back bent. Finally, as an application, we used our deformation method to generate different body types, performed forward dynamics simulations in an assistive device setting and visualized the differences in contact pressure distributions due to body shape changes.**

I. Introduction

Modeling human body shape is an important problem in many fields, such as virtual fitting for fashion industry, computer animation and design of assist devices. A common way to do this is to acquire 3D scans of human body surfaces using laser range scanners and construct a statistical model of human body shape from the resulting 3D scans.

The first work in this line of research was done by Allen et al. [1] where the authors fit a template 3D body model to Caesar dataset that contains a couple of thousand subjects and used principal component analysis (PCA) to model the space of human body shape. Later, several techniques are proposed to extend the method of Allen et al. to handle both body shape and pose variations (such as SCAPE [2] and SMPL [3]) and even dynamic deformations (e.g., FAUST [8]).

One of the difficulties in the use of a statistical model of 3D human body shape is that it is limited by the subjects included in the dataset. For example, Caesar dataset, the most common human body shape dataset, contains the subjects whose ages are in the range of 18-65. In general, publicly available dataset do not include children and elderly people. Park and Reed built a statistical parametric body shape model of children in ages between 3 and 11 years [7]. Recently Hesse et al. [4] proposed a technique to capture body shape and pose of moving infants using a 3D vision sensor. On the other hand, we focus on constructing a body shape model including elderly people.

[1]Yusuke Yoshiyasu, Vincent Samy, Yumeko Imamura, Ko Ayusuwa, Ryuusuke Sagawa and Eiichi Yoshida are with National Institute of Advanced Industrial Science and Technology (AIST) and CNRS-AIST JRL (Joint Robotics Laboratory) UMI3218/IRL, Japan. {yusuke-yoshiyasu}@aist.go.jp

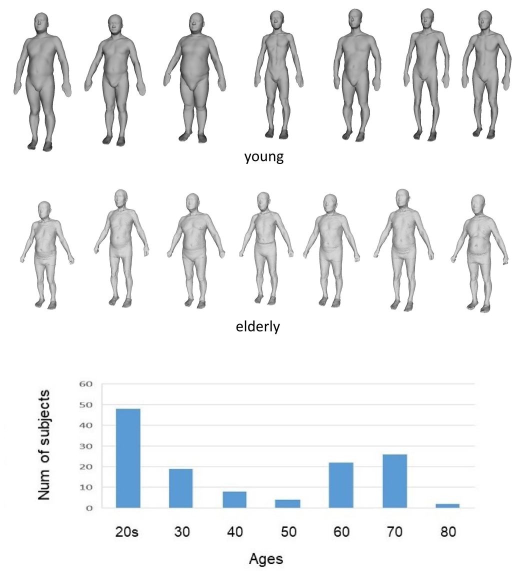

Fig. 1. Top: Some examples of young-age and elderly subjects from human body shape dataset. Bottom: the numbers of subjects in the age ranges.

In this paper, we establish a statistical human model that includes elderly people. Here we are not aiming at constructing a large dataset. Instead we intend to extract characteristics of elderly body shapes and investigate the effects when incorporating elderly subjects in the body shape dataset. One difficulty in doing so is that the poses of 3D scans are different to each other as we combine the data which may be acquired in different experiment settings. To solve this, we fit a template mesh model to 3D scan data using a coarse-to-fine surface registration technique that takes into account pose variations. First, the pose is aligned using a skeleton based deformation technique. Then, the correspondences between the scans of different subjects are established finely based on a conformal mapping deformation method. By performing principal component analysis (PCA) and mapping PC scores to a small set of parameters such as "age", "weight" and "height" or the measurable anthropometric parameters like "shoulder width", it is possible to easily change the body shape with these parameters. We also designed a simple user interface to perform deformation using this model. Finally we showed an application of human body shape statistical model to forward dynamics of human figures interacting with

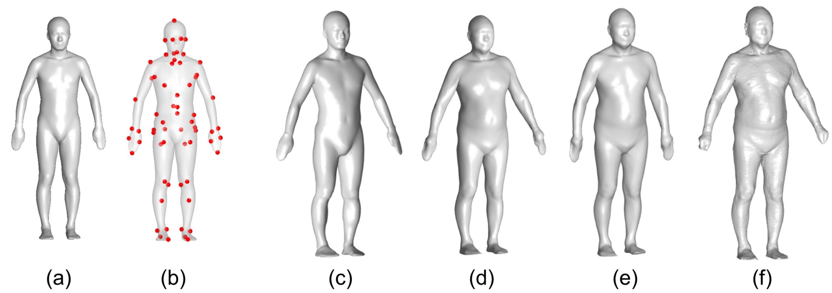

Fig. 2. Overview of our coarse-to-fine surface registration. (a) Template, (b) marker placement definition, (c) skeleton fitting result, (d) surface registration result, (e) final pose corrected result and (f) target 3D scan surface.

assist devices and visualized contact pressure distributions.

II. TEMPLATE FITTING TO WHOLE-BODY 3D SCANS

A. Data acquisition

Human whole-body 3D scans are acquired and collected by AIST Digital Human Engineering Research Center. From this dataset we used the 3D scans of $N \approx 130$ male subjects (including about 50 elderly over 65) where the ages of the subjects are shown in Fig. 1 bottom. Note that mesh smoothing is performed on the faces of 3D scans to remove surface details to ensure protection of subjects' privacy.

B. Coarse-to-fine surface registration

In order to construct a statistical model from 3D scans, we establish correspondences between them—this is a preprocessing step to know which points on one scan corresponds to the points on different scans (e.g., the ear to ear and the toe to toe). This process is done by fitting a generic template human mesh model to 3D scans.

The overview of our registration approach is depicted in Fig. 2. To establish correspondences, a template mesh model (Fig. 2 (a)) was fitted to 3D scan data (Fig. 2 (f)). Since 3D scans are coming from different experiments and their poses are possibly different to each other, we take a coarse-to-fine approach that first aligns skeletal pose (Fig. 2 (c)) and then shape (Fig. 2 (d)). The final mesh is obtained by transforming back the deformed mesh to the rest pose (Fig. 2 (e)).

A template mesh is modeled as a triangle mesh that contains n and m triangle faces. The positions of the template, $\mathbf{v}_1 \dots \mathbf{v}_n$, are denoted by a $n \times 3$ vector, $\mathbf{v} = [\mathbf{v}_1 \dots \mathbf{v}_n]^{\mathrm{T}}$. In this work the number of vertices is approx. 8000 vertices. The registration is expressed as a set of 3×4 affine transformation matrices $\mathbf{X}_i$ that are associated with each vertex of the template mesh, $\mathbf{X} = [\mathbf{X}_1 \dots \mathbf{X}_n]$.

Conformal deformation We use the as-conformal-as-possible deformation approach [10] to deform a template model in both skeleton fitting and fine-scale shape deformation. This method attains angle-preserving mappings and constrains the transformations of the model as similarity transformations (scale + rotation) locally as much as possible, which allows us to fit the model to the target geometry in a flexible way while preserving the mesh structure with

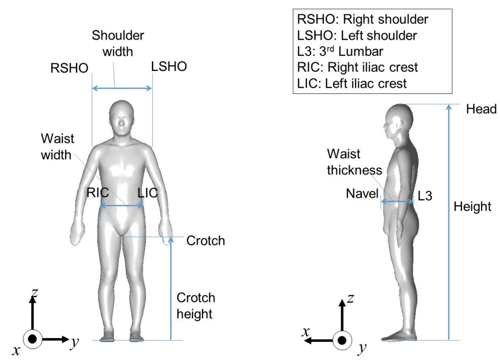

Fig. 3. Measurement items.

less distortions. The cost function is defined as follows:

$$\begin{aligned} E(\mathbf{X}) = & \, w_{\mathrm{ASAP}} E_{\mathrm{ASAP}}(\mathbf{X}) \\ & + w_{\mathrm{Closest}} E_{\mathrm{Closest}}(\mathbf{X}) \\ & + w_{\mathrm{Marker}} E_{\mathrm{Marker}}(\mathbf{X}) \end{aligned} \quad (1)$$

where E_{ASAP} constrains deformation as-similar-as-possible, which equivalently achieves conformal mappings, and E_{Closest} penalizes distances between the closest points of template and target surface. The closest points from the model and the target 3D scanned points are found by the nearest neighbor search based on kd-tree. E_{Marker} is the positional constraint anatomical landmarks, which attracts the template mesh vertices corresponding to the landmarks toward the measured landmarks. Here we provide approximately 60 anatomical feature points for marker correspondences (Fig. 2 (b)). The energy is minimized using the alternating optimization technique where the first step optimizes the vertex positions with fixed transformations and the second step optimizes affine transformations with fixed vertex positions.

Pose alignment Since the pose of the subject is different from that of the template, it needs to be aligned before surface registration (Fig. 2 (c)). To do so, we use skinning (aka., skeletal subspace deformation or linear blend skinning). Each vertex in the dense mesh is assigned skinning weights and its deformed position is computed from bone transformations. Instead of assigning an affine transformation to each vertex we define it at each skeletal joint.

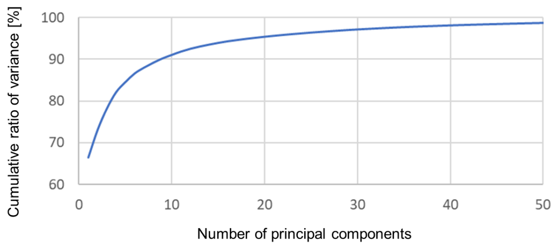

Fig. 4. The cumulative ratio of variance [%] for the first 50 principle components. It reaches approx. 92% at 10 PC and approx. 99% at 50 PC.

Skinning computes vertex positions from the joint transformations. Let us define the joint positions of the skeleton as $\mathbf{j}_k$. The linear transformation and the translation associated with $\mathbf{j}_k$ is denoted by $\mathbf{T}_k$ and $\mathbf{t}_k$, respectively. Let $\mathbf{j}_k^0$ be the joint position of the skeleton in the rest state. The deformed vertex is obtained as follows:

$$\bar{\mathbf{v}}_i = \sum_{k=1}^{c} w_i^{(k)} [\mathbf{T}_k(\mathbf{v}_i^0 - \mathbf{j}_k^0) + \mathbf{j}_k^0 + \mathbf{t}_k] \tag{2}$$

where c is the number of joints in the skeleton. $w_i^{(k)}$ is a weight for vertex i, controlling how much $\mathbf{v}_i$ is influenced by $\mathbf{j}_k$. Consequently, given scan-template correspondences $\mathcal{C} = \{(\mathbf{v}_1, \mathbf{p}_{\mathrm{idx}(1)}) \dots (\mathbf{v}_n, \mathbf{p}_{\mathrm{idx}(n)})\}$, where $\mathrm{idx}(i)$ is the index of the scan point that is matched with vertex i, we can define the correspondence energy by minimizing the skinned vertex position $\bar{\mathbf{v}}_i$ and the closest points as:

$$E_{\mathrm{Closest}} = \sum_{i \in \mathcal{C}} \|\bar{\mathbf{v}}_i - \mathbf{p}_{\mathrm{idx}(l)}\|^2 \tag{3}$$

Fine-scale deformation After aligning skeletal poses by optimizing the affine transformations of skeletons, we perform surface registration by optimizing affine transformations assigned to vertices (Fig. 2 (d)). Finally, the pose of registered surface is transformed back to the rest pose (Fig. 2 (e)).

III. Statistical body shape model and low dimensional parametrization

A. Principal component analysis (PCA)

To construct a statistical body shape model, we use the whole body shape dataset that is a collection of 3D models in mutual correspondences established in the previous section. The models are compressed into a low dimensional basis using principal component analysis (PCA). In order to construct a PCA body model, the three coordinates of vertices for subject j is stacked into a column vector as:

$$\mathbf{s}_j = [x_{1,j}, y_{1,j}, z_{1,j} \dots x_{n,j}, y_{n,j}, z_{n,j}]^T \tag{4}$$

$\mathbf{s}_j$ is assembled for all individual to get shape matrix $\mathbf{S} \in \mathbb{R}^{3n \times N}$. PCA is applied on $\mathbf{S}$ to obtain mean shape $\mathbf{m}$ and a set of eigenvectors $\mathbf{U}$. Note that we perform PCA on the covariance matrix of $\mathbf{S}$ without standardization because it preserves scale and, in our problem, input data have the

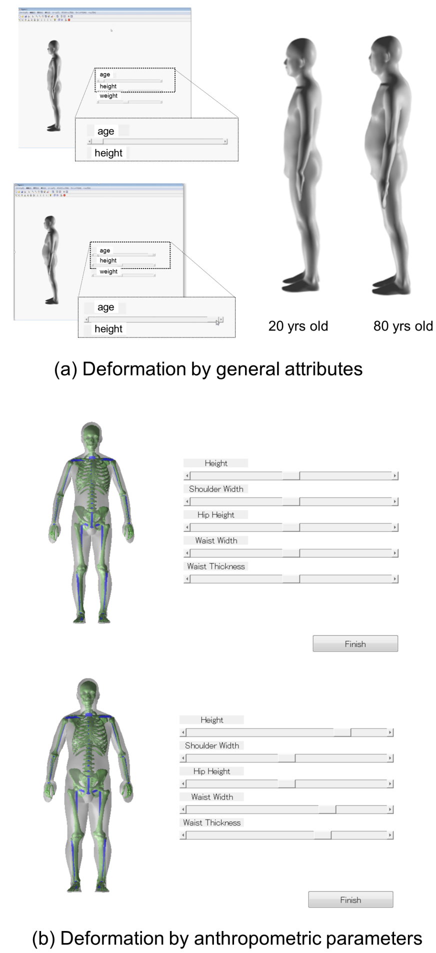

Fig. 5. User interface and body shape deformation results.

same unit and similar scale [1]. Reconstruction of the vertex position of a body shape from eigenvectors is achieved as:

$$\mathbf{s}_j = \mathbf{U}\mathbf{w}_j + \mathbf{m} \tag{5}$$

where $\mathbf{w}_j$ is the weight of principal components (PC scores) for subject j. In Fig. 4, we showed the cumulative ratio of variance for the first 50 principle components. It reaches approx. 92% at 10 PC and approx. 99% at 50 PC. Since more than 90% of the original data is explained by the first ten components and the variance is already close to zero when reaching to around the 7th components, we decided to keep the first ten principal components.

B. Body shape deformation with a small set of parameters

Altering PC scores directly is however not intuitive to change body shapes for a practical use. We therefore provide two ways for deforming body shape using a small set of parameters: 1) general attributes, such as age and height, and 2) anthropometric parameters which can be measured using a ruler and anthropometer.

Deformation with general attributes In order to change the body type by three parameters "age", "weight" and "height", a linear transformation between these attributes

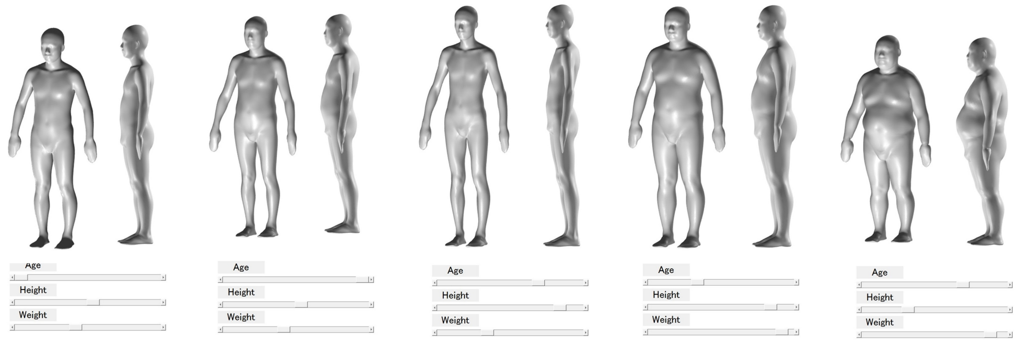

Fig. 6. Different body types generated by our method. By reproducing the body form of the elderly using this method, we were able to generate a style capturing the characteristics of elderly people whose shoulders fell and the back was bent (the first column vs the second column).

and the principal component scores are obtained by linear regressions following Allen et al. [1].

Let $\mathbf{a} = [a_1, a_2, a_3, 1]^T$ be an attribute vector containing "age", "weight" and "height". Suppose we have the linear mapping $\mathbf{M} \in \mathbb{R}^{10\times(3+1)}$ that maps attribute vector $\mathbf{a}$ to PC scores $\mathbf{w}$. Given attribute vector $\mathbf{a}$, the new weight $\tilde{\mathbf{w}}$ is computed by $\tilde{\mathbf{w}} = \mathbf{Ma}$. The new body shape is then obtained by substituting $\tilde{\mathbf{w}}$ into Eq. 5, i.e., $\tilde{\mathbf{s}} = \mathbf{U}\tilde{\mathbf{w}} + \mathbf{m}$. Using $\mathbf{M}$, we can thus easily change body shape by an arbitrary set of general attributes.

Our remaining task here is to obtain linear mapping $\mathbf{M}$ from the set of attributes and PC scores obtained from the body shape dataset. Let $\mathbf{A} \in \mathbb{R}^{(3+1)\times N}$ and $\mathbf{P} \in \mathbb{R}^{10\times N}$ be the matrices containing general attributes and principal component scores for all the subjects, respectively. The linear mapping $\mathbf{M}$ is then calculated as $\mathbf{M} = \mathbf{PA}^+$ where $\mathbf{A}^+$ is the pseudo inverse of $\mathbf{A}$.

Deformation with anthropometric parameters Here, to deform body shape with anthropometric parameters we propose a method that is inspired by the subspace linear deformation model [5] using the PCA body model as a subspace. In this way, the body model can be deformed more exactly than linear regressions by imposing length constraints directly on the body model. To make a method computationally efficient, we use linear constraints, which means that a set of measurement parameters must be parallel (or perpendicular) to the canonical coordinate frame. Note that, using non-linear deformation model like mass spring systems [6], this method can be extended to use measurement items that are not parallel to the canonical frame.

Considering also the ease of measurement we chose the measurement items as in Fig. 3, i.e., height (h), shoulder width (w_s), waist width (w_w), waist thickness (t_w) and crotch height (h_c), which can be calculated as the distance between the following point:

$$\begin{aligned} h &= z_{\text{head}} \\ w_s &= y_{\text{LSHO}} - y_{\text{RSHO}} \\ w_w &= y_{\text{LIC}} - y_{\text{RIC}} \\ t_w &= x_{\text{navel}} - x_{\text{L3}} \\ h_c &= z_{\text{Crotch}} \end{aligned} \tag{6}$$

where the definition of the landmarks are defined in Fig. 3. Let $\mathbf{e}$ be a vector containing the measurement items, $\mathbf{e} = [h, w_s, w_w, t_w, h_c]$. Then, Eq. 6 can be rewritten in the matrix form as: $\mathbf{e} = \mathbf{Gs} = \mathbf{G}(\mathbf{Uw} + \mathbf{m})$, where $\mathbf{G} \in \mathbb{R}^{5\times n}$ is an incident matrix containing 1 and -1. Consequently, we can obtain the new coefficients $\tilde{\mathbf{w}}$ in a least squares sense so that the body shape conforms with the measurement parameters, by solving the following normal equation:

$$\tilde{\mathbf{w}} = (\mathbf{G}^T\mathbf{G})^{-1}\mathbf{G}^T(\mathbf{e} - \mathbf{Gm}) \tag{7}$$

By taking advantage of the fact that the directions of the measurement items are parallel to the canonical coordinate frame axes, Eq. 7 can be solved linearly, which is efficient. Again, the new body shape is obtained by solving Eq. 5 with $\tilde{\mathbf{w}}$.

IV. Results and Applications

A. Interactive body shape deformation using GUI

In Figs. 5 and 6, we show different body types generated by our method. As a result of reproducing the body form of the elderly using this method, we were able to produce a body style capturing the characteristics of elderly people whose shoulders fell and the back bent (Fig. 5 (a)).

B. Evaluation of body shape reconstruction techniques

In Fig. 7, we visualized the reconstruction error using the first 10 PC scores. We measured the distance between the deformed template and reconstructed shape at each vertex. Mostly, the average reconstruction error is below 10 mm. Occasionally, there are regions with large errors over 50 mm, which is probably due to pose differences of the left and right hands, as the PCA reconstruction usually symmetrizes the shape.

We also evaluated the results obtained using the deformation method based on general attributes (Fig. 8). In this case, the control parameters are only three: "age", "height" and "weight", which is very challenging problem. As can be seen from Fig. 8, large errors are found around hands and feet, as this deformation model cannot change the arm and leg length independently. However, considering the error range of reconstruction results using the first 10 PC scores

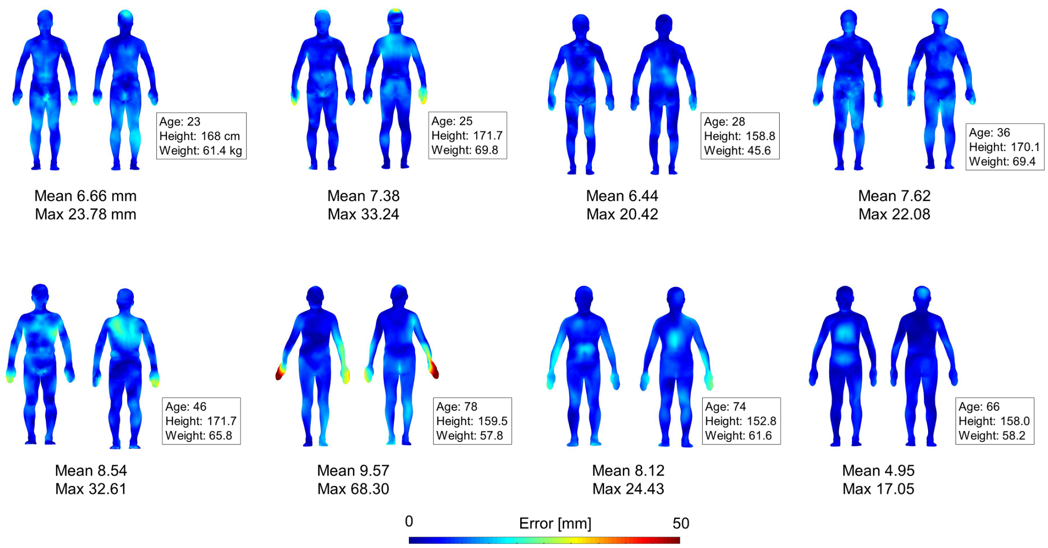

Fig. 7. PCA reconstruction error. We measured the distance between the deformed template and reconstructed shape using 10 PC scores at each vertex. For each body model, the left and right are the visualization of the error for the front and back side, respectively. The numbers below are the mean error [mm] and maximum error [mm] are also shown.

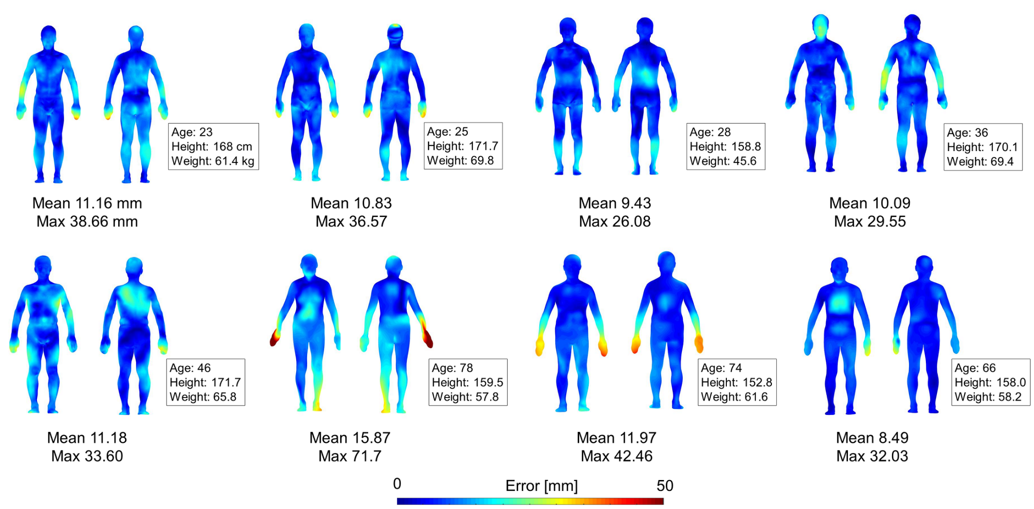

Fig. 8. Reconstruction errors of deformation results by general attributes. We measured the distance between the deformed template and reconstructed shape using the deformation method based on “age”, “height” and “weight”. The numbers below are the mean error [mm] and maximum error [mm] are also shown.

(Fig. 7), we believe that the results are in the acceptable range for our application i.e., to roughly make the characteristics of elderly people’s body shape visible and to perform forward dynamics simulations in an assistive device setting.

C. Application to forward dynamics simulation

As an application, we applied our body shape deformation technique to generate forward dynamics simulations of different body types. We performed simulation of a sling lift assistive device in contact with a human body model, where the sheet is modeled using simple mass spring systems. This device is designed to support transfer, for example, from a bed to a wheel chair.

For the forward dynamics model we used the method presented in [9]. Here the skeleton is modeled as an open-loop tree structure with the root joint at the hip. We describe a pose of the skeleton using the generalized coordinates $\mathbf{q}$, which includes joint angles of the skeleton, the absolute position and orientation of the root joint.

To apply the simulation technique to different body types, we alter physical properties of segments according to body deformation based on a simple approximation model. Once the body shape has been changed, the mass, center of mass (COM) and inertia of segments are modified. We approximate deformation with anisotropic scalings of segments (s_x, s_y and s_z) and apply the changes in physical properties

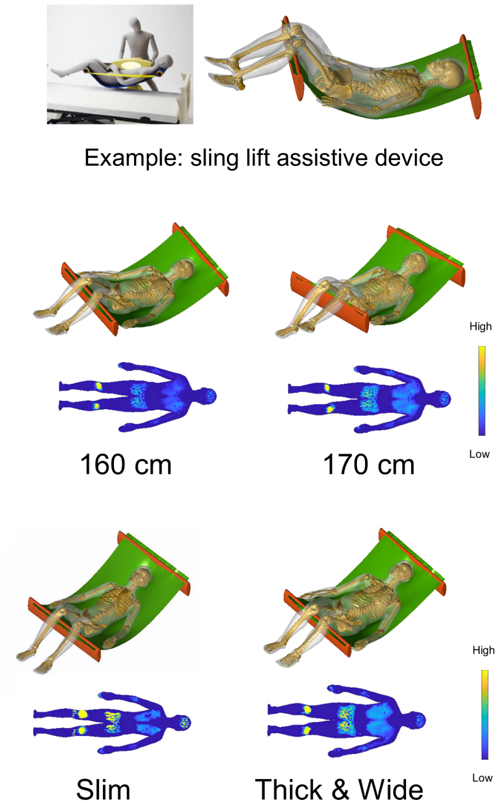

Fig. 9. Simulation results of a simple model of sling lift assistive device in contact with a human body model. We performed simulations by varying height (160cm and 170cm) as well as shoulder width and waist width/thickness (Slim and Thick&Wide). Contact force estimation results are shown under the visualizations of human figure model.

as follows. Let m, $\mathbf{c}$ and $\mathbf{I}$ be the original mass, COM and inertia of segments, respectively. Then subject specific physical properties $\tilde{m}$, $\tilde{\mathbf{c}}$ and $\tilde{\mathbf{I}}$ can be calculated as:

$$\tilde{m} = m \cdot \tilde{V}/V = m \cdot s_x \cdot s_y \cdot s_z \tag{8}$$

$$\tilde{\mathbf{c}} = \begin{bmatrix} s_x & 0 & 0 \\ 0 & s_y & 0 \\ 0 & 0 & s_z \end{bmatrix} \mathbf{c} \tag{9}$$

$$\tilde{\mathbf{I}} = \begin{bmatrix} s_x^2 \cdot I_{xx} & s_x \cdot s_y \cdot I_{xy} & s_x \cdot s_z \cdot I_{xz} \\ s_y \cdot s_x \cdot I_{yx} & s_y^2 \cdot I_{yy} & s_y \cdot s_z \cdot I_{yz} \\ s_z \cdot s_x \cdot I_{zx} & s_z \cdot s_y \cdot I_{yz} & s_z^2 \cdot I_{zz} \end{bmatrix} \tag{10}$$

where V and $\tilde{V}$ are the volumes of a segment before and after deforming a body shape.

Fig. 9 shows simulation results on different body types and visualizations of their contact force estimations. Here, we performed simulations by varying height (160cm and 170cm) as well as shoulder width and waist width/thickness (Slim and Thick&Wide). Contact force estimation results among different body types show visual differences between them. For example, the estimated contact forces of the body model with height 160cm are concentrates around knee. This is probably because the body is not well supported by the buttocks due to its short legs (especially short thighs). Also, the estimated contact forces of the slim body model are higher at the knees and buttocks than that of the thick and wide body model, since the body surface area contacting with the sheet is smaller. Note that the results resembles with the tactile sensor measurements [9].

V. Conclusion

We presented a statistical body shape model that includes elderly people using PCA. As a pre-processsing step, the coarse-to-fine registration technique is proposed to establish correspondence between 3D scans. We also introduced the body deformation model using a small set of parameters and a simple graphical user interface to change body shapes easily. The proposed body deformation method was applied to forward dynamics simulation of an assistive device interacting with a human model to examine different body types. In future work, we would like to address the modeling of material properties such as skin tissue and joint stiffness.

Acknowledgments

We would like to thank Makiko Kouchi and Masaaki Mochimaru for providing us the 3D body scan dataset.

References

[1] B. Allen, B. Curless, and Z. Popović, "The space of human body shapes: reconstruction and parameterization from range scans," *ACM Trans. Graph.*, vol. 22, no. 3, pp. 587–594, 2003.

[2] D. Anguelov, P. Srinivasan, D. Koller, S. Thrun, J. Rodgers, and J. Davis, "Scape: shape completion and animation of people," *ACM Trans. Graph.*, vol. 24, pp. 408–416, 2005.

[3] F. Bogo, A. Kanazawa, C. Lassner, P. Gehler, J. Romero, and M. J. Black, "Keep it smpl: Automatic estimation of 3d human pose and shape from a single image," in *ECCV*. Springer, 2016, pp. 561–578.

[4] N. Hesse, S. Pujades, J. Romero, M. J. Black, C. Bodensteiner, M. Arens, U. G. Hofmann, U. Tacke, M. Hadders-Algra, R. Weinberger, W. Müller-Felber, and A. S. Schroeder, "Learning an infant body model from RGB-D data for accurate full body motion analysis," in *International Conference on Medical Image Computing and Computer-Assisted Intervention (MICCAI)*, 2018.

[5] J. Huang, X. Shi, X. Liu, K. Zhou, L.-Y. Wei, S.-H. Teng, H. Bao, B. Guo, and H.-Y. Shum, "Subspace gradient domain mesh deformation," July 2006.

[6] T. Liu, A. W. Bargteil, J. F. O'Brien, and L. Kavan, "Fast simulation of mass-spring systems," *ACM Transactions on Graphics*, vol. 32, no. 6, pp. 209:1–7, Nov. 2013, proceedings of ACM SIGGRAPH Asia 2013, Hong Kong.

[7] B.-K. Park and M. P. Reed, "Parametric body shape model of standing children aged 311 years," *Ergonomics*, vol. 58, no. 10, pp. 1714–1725, 2015, pMID: 25933223.

[8] G. Pons-Moll, J. Romero, N. Mahmood, and M. J. Black, "Dyna: A model of dynamic human shape in motion," *ACM Transactions on Graphics, (Proc. SIGGRAPH)*, vol. 34, no. 4, pp. 120:1–120:14, Aug. 2015.

[9] Y. Yoshiyasu, K. Ayusawa, E. Yoshida, Y. Matsumoto, and Y. Endo, "Forward dynamics simulation of human figures on assistive devices using geometric skin deformation model," in *2015 37th Annual International Conference of the IEEE Engineering in Medicine and Biology Society (EMBC)*, Aug 2015, pp. 2442–2445.

[10] Y. Yoshiyasu, W.-C. Ma, E. Yoshida, and F. Kanehiro, "As-conformal-as-possible surface registration," *Comput. Graph. Forum*, vol. 33, no. 5, pp. 257–267, 2014. [Online]. Available: http://dx.doi.org/10.1111/cgf.12451